

Mapping Allostery through Equilibrium Perturbation NMR Spectroscopy

Rahul Das, Mona Abu-Abed, and Giuseppe Melacini*

Department of Biochemistry and Biomedical Sciences and Department of Chemistry, McMaster University,
1280 Main Street West, Hamilton, ON L8S 4M1, Canada

Received January 3, 2006; E-mail: melacin@mcmaster.ca

Allostery is a fundamental mechanism for regulating biological function through ligand binding.¹ While understanding the structural basis of allosteric control relies on the comparative analysis of macromolecules in their free and bound states, the direct free versus bound comparison is often experimentally challenging due to the instability of one of the two forms.² This is the case for the regulatory subunit (R) of the prototypical and ubiquitous protein kinase A (PKA), which is the main eukaryotic receptor for the cAMP second messenger.³ The cyclic-nucleotide binding (CNB) domain of R that interacts with and allosterically controls the PKA catalytic subunit (C) is poorly soluble in its free form, and as a result, only limited information is currently available at residue or atomic resolution for the *apo* state of this ancient CNB module,³ despite its relevance for both signaling and the cyclic nucleotide dependent allostery in general.^{3–6} Analogous experimental challenges frequently hinder the comparative analysis of both prokaryotic and eukaryotic macromolecules in the *apo* and *holo* states because often one of the two forms is aggregation prone due to the exposure of hydrophobic patches upon ligand binding or release.^{2,4,5,7}

Here we propose a general experimental strategy based on equilibrium perturbation NMR to effectively circumvent the drawbacks intrinsic to direct *apo/holo* comparisons. The proposed method takes advantage of the ability of recently developed NMR relaxation dispersion (NMRD)^{8,9} experiments as well as of hydrogen exchange (H/D and H/H) measurements^{10,11} to probe (“spy”) with high sensitivity minimally populated states within dynamic conformational equilibria. As a result, the experimentally challenging direct free/bound comparison can be replaced by another more easily implemented comparison, namely, between one solution in which the protein is prepared in its most stable state (either free or bound depending on the specific system under investigation) and another solution in which the equilibrium is slightly perturbed by introducing a minor population of the least stable form of the protein. The reduced effective concentration of the unstable state and the continuous on/off ligand exchange ensure the stability of the second solution. In this sample, the direct detection of the least stable form is ineffective due to its low population, but it can still be indirectly investigated by NMRD and hydrogen exchange experiments.

The effectiveness of the proposed equilibrium perturbation NMR approach is illustrated here through its application to the CNB domain that serves as the central controlling unit of the isoform I α of PKA (RI α (119–244)).^{3,12} RI α (119–244) includes a highly conserved structural module, and it represents a good model for CNB domains in general.^{3–6,12,13} We therefore prepared two samples of RI α (119–244): in one, the *holo* state was stabilized by the addition of a 10-fold excess of cAMP, and in the other, a minor (<10–20%) population of the *apo* form was created by removing excess free cAMP through dialysis under non-denaturing conditions (Supporting Information). No detectable ¹H and ¹⁵N amide chemical shift differences between the cAMP saturated and unsaturated

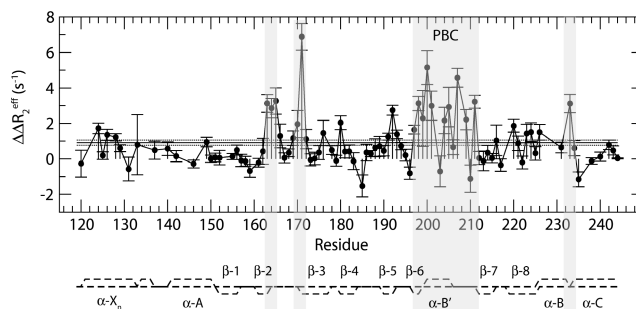


Figure 1. Effect of the equilibrium perturbation on the backbone ¹⁵N relaxation dispersion (ΔR_2^{eff}) measured for RI α (119–244). $\Delta\Delta R_2^{\text{eff}}$ is the difference between the relaxation dispersion measured before and after the addition of 1 mM cAMP to 0.1 mM RI α (119–244) dialyzed under non-denaturing conditions to remove excess unbound cAMP (Supporting Information, Figures S2 and S3). The R_2^{eff} rates were measured at 309 K (50 mM MES, pH 6.5, 100 mM NaCl and 0.02% NaN₃), and $\Delta\Delta R_2^{\text{eff}}$ was computed according to equations S2–S5 (Supporting Information).⁸ All data were acquired at 700 MHz with a TCI cryo-probe. Additional experimental details are available in the Supporting Information. The dashed lines below the graph indicate the 2° structure expected based on the coordinates for the cAMP-bound regulatory subunit of PKA.³ The horizontal lines on the graph indicate the average $\Delta\Delta R_2^{\text{eff}}$ value \pm the standard error. “PBC” denotes the cAMP binding site. The other gray regions indicate allosteric sites previously hypothesized based on mutant and sequence analyses.¹³

proteins were observed in the HSQC spectra (Figure S4), but both solutions were stable, thus enabling NMRD measurements for both samples. Specifically, the ¹⁵N relaxation dispersion (ΔR_2^{eff}) was measured using relaxation-compensated constant-time (RC-CT) CPMG experiments⁸ at CPMG field strengths (ν_{CPMG}) of 43 and 472 Hz (Supporting Information). Since the on/off ligand exchange occurs in the ~1 to ~100 ms time scale, as indicated by the ROESY analysis (Figure S1), the difference in ΔR_2^{eff} ($\Delta\Delta R_2^{\text{eff}}$) between the two samples (Figure 1) is a sensitive indicator of residues affected by nucleotide binding. This is confirmed by several higher than average $\Delta\Delta R_2^{\text{eff}}$ values observed in Figure 1 for residues 199–211, which comprise the known cAMP binding site of RI α (119–244) (phosphate binding cassette, PBC). Figure 1 also shows that the effect of cAMP binding propagates well beyond the PBC as expected for an extended nucleotide-dependent allosteric network of interactions. The allosteric “hot spot” map revealed by the $\Delta\Delta R_2^{\text{eff}}$ measurement is fully consistent with existing independent hypotheses on the cAMP allostery based on site-directed mutagenesis as well as sequence analyses.^{5,13,14} For instance, the cluster of higher than average $\Delta\Delta R_2^{\text{eff}}$ values localized at the end of the β_2 strand (Figure 1) confirms the hypothesis based on surface matching¹³ that identifies this region as a highly conserved secondary hydrophobic layer required for the stability of CNB domain–cAMP complexes.¹³ Similarly, the peak $\Delta\Delta R_2^{\text{eff}}$ values observed at the beginning of the β_3 strand (Figure 1) are fully consistent with the observation that the D170A mutant is non-

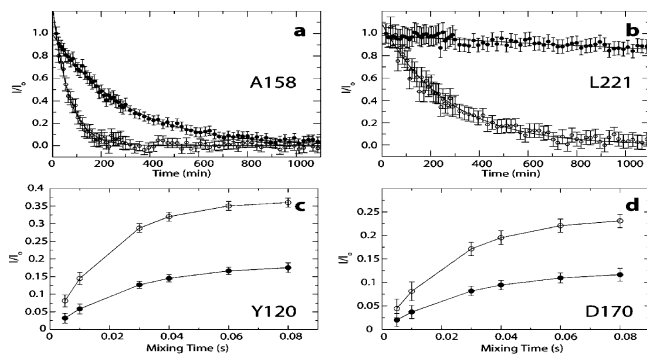


Figure 2. Effect of the equilibrium perturbation on H/D (a, b) and H/H (c, d) exchange rates for representative backbone amide protons of RI α (119–244).^{10,11} Open and filled circles, respectively, refer to data measured before and after addition of 1 mM cAMP to 0.1 mM RI α (119–244) dialyzed under nondenaturing conditions to remove excess unbound cAMP (Supporting Information). Other experimental conditions are as in Figure 1. Further details are available as Supporting Information.

losteric, even though it preserves high binding affinity for both cAMP and the catalytic (C) subunit of PKA.¹⁴ This result highlights the importance of the D170–R209 interaction within the allosteric network that mediates the cross-talk between the cAMP and the C binding sites of RI α . In addition, the higher than average $\Delta\Delta R_2^{\text{eff}}$ value measured for L233 located at the interface between the B- and C-helices confirms the previously proposed hypothesis on the cAMP-controlled repositioning of the kinase-interacting C-helix through hydrophobic hinge motions.^{3,5,13} Overall, the consistency between the results of Figure 1 and previous independent mutational and computational analyses corroborates the usefulness of the equilibrium perturbation NMRD approach for identifying residues involved in binding and allosteric networks.

Further insight about the nature of the conformational transitions controlled by ligand binding is obtained by extending the equilibrium perturbation method to other types of experiments that are sensitive to minor populations within dynamic equilibria. These include hydrogen exchange (H/D and H/H) measurements that provide information complementary to the NMRD data (Figure 1). Whereas the ΔR_2^{eff} enhancements of Figure 1 mainly reflect chemical shift variations between the *apo* and *holo* forms in their most stable states,^{8,9} the differences in the hydrogen exchange rates between the free and bound protein probe primarily how the ligand perturbs the more excited, partially unfolded and exchange competent conformers within the free energy landscape. To fully evaluate the role of a ligand in remodeling the free energy landscape, it is therefore critical to assess its effect also on the hydrogen exchange rates. For this purpose, the equilibrium perturbation approach is extremely useful as shown in Figure 2a,b, which illustrates how even minor variations in the relative *apo/holo* populations as those employed for the $\Delta\Delta R_2^{\text{eff}}$ measurements generate marked changes in the hydrogen exchange rates monitored in real time through H/D exchange experiments.¹⁰ The equilibrium perturbation method is not only instrumental in effectively circumventing the experimental problems associated with the direct determination by NMR of the exchange rates for the aggregation prone *apo* state of RI α (119–244), but it also provides the additional advantage of increasing the number of detectable fast exchanging amide protons that in the pure *apo* state would have been fully exchanged within the dead time of the H/D experiment. Furthermore, if the hydrogen exchange is too rapid to be monitored even

by equilibrium perturbation real-time H/D measurements, it can often be probed by H/H exchange pulse sequences, such as the CLEANEX-PM (Figure 2c,d).¹¹ Again, as shown in Figure 2c,d, the observation of the effect of ligand binding on the H/H exchange rates is critically enabled by the equilibrium perturbation strategy.

In summary, we have shown that the equilibrium perturbation NMR approach is an effective method to map ligand binding and allostery, avoiding the problems frequently associated with the direct comparison of the ligand free versus bound states, as often only one of the two states is stable and amenable to direct experimental characterization. Minor *apo/holo* equilibrium perturbations are tolerated without compromising sample stability and can still reveal relevant *apo/holo* differences if monitored through suitable NMR experiments, such as NMRD as well as H/D and H/H exchange. Together these complementary measurements help unveil how a ligand affects both the stable and the excited states within the free energy landscape of its protein receptors. We conclude that the equilibrium perturbation approach significantly expands the scope of applicability of NMRD and hydrogen exchange experiments to the investigation of ligand–protein interactions in general, unmasking allosteric maps for systems that have been traditionally elusive to direct free/bound comparisons.

Acknowledgment. We thank Dr. S. S. Taylor for making the RI α (119–244) clone available and, together with Dr. L. E. Kay and Dr. A. Bain, for helpful discussions. We are grateful to the Canadian Institutes of Health Research for financial support.

Supporting Information Available: Materials and methods details. This material is available free of charge via the Internet at <http://pubs.acs.org>.

References

- (1) (a) Kern, D.; Zuiderweg, E. R. P. *Curr. Opin. Struct. Biol.* **2003**, *13*, 748. (b) Volkman, B. F.; Lipson, D.; Wemmer, D.; Kern, D. *Science* **2001**, *291*, 2429.
- (2) (a) Won, H. S.; Lee, T. W.; Park, S. H.; Lee, B. J. *J. Biol. Chem.* **2002**, *277*, 11450. (b) Kraemer, A.; Rehmann, H. R.; Cool, R. H.; Theiss, C.; de Rooij, J.; Bos, J. L.; Wittinghofer, A. *J. Mol. Biol.* **2001**, *306*, 1167.
- (3) (a) Kim, C.; Xuong, N. H.; Taylor, S. S. *Science* **2005**, *307*, 690. (b) Su, Y.; Dostmann, W. R. G.; Herberg, F. W.; Durick, K.; Xuong, N. H.; Teneyck, L.; Taylor, S. S.; Varughese, K. I. *Science* **1995**, *269*, 807. (c) Anand, G. S.; Hughes, C. A.; Jones, J. M.; Taylor, S. S.; Komives, E. A. *J. Mol. Biol.* **2002**, *323*, 377. (d) Wu, J.; Brown, S.; Xuaong, N. H.; Taylor, S. S. *Structure* **2004**, *12*, 1057.
- (4) (a) Weber, I. T.; Steitz, T. A. *J. Mol. Biol.* **1987**, *198*, 311. (b) Parkinson, G.; Wilson, C.; Gunasekera, A.; Ebright, Y. W.; Ebright, R. E.; Berman, H. M. *J. Mol. Biol.* **1996**, *260*, 395.
- (5) Rehmann, H.; Prakash, B.; Wolf, E.; Rueppel, A.; De Rooij, J.; Bos, J. L.; Wittinghofer, A. *Nat. Struct. Biol.* **2003**, *10*, 26.
- (6) (a) Clayton, G. M.; Silverman, W. R.; Heginbotham, L.; Morais-Cabral, J. H. *Cell* **2004**, *119*, 615. (b) Zagotta, W. N.; Olivier, N. B.; Black, K. D.; Young, E. C.; Olson, R.; Gouaux, E. *Nature* **2003**, *425*, 200.
- (7) Fayos, R.; Melacini, G.; Newlon, M. G.; Burns, L.; Scott, J. D.; Jennings, P. A. *J. Biol. Chem.* **2003**, *278*, 18581.
- (8) (a) Tollinger, M.; Skrynnikov, N. R.; Mulder, F. A. A.; Forman-Kay, J. D.; Kay, L. E. *J. Am. Chem. Soc.* **2001**, *123*, 11341. (b) Mulder, F. A. A.; Skrynnikov, N. R.; Hon, B.; Dahlquist, F. W.; Kay, L. E. *J. Am. Chem. Soc.* **2001**, *123*, 967.
- (9) (a) Palmer, A. G.; Kroenke, C. D.; Loria, J. P. *Methods Enzymol.* **2001**, *339*, 204. (b) Eisenmesser, E. Z.; Bosco, D. A.; Akke, M.; Kern, D. *Science* **2002**, *295*, 1520. (c) Malmendal, A.; Evenas, J.; Forsen, S.; Akke, M. *J. Mol. Biol.* **1999**, *293*, 883.
- (10) Bai, Y. W.; Englander, J. J.; Mayne, L.; Milne, J. S.; Englander, S. W. *Methods Enzymol.* **1995**, *259*, 344.
- (11) (a) Hwang, T. L.; van Zijl, P. C. M.; Mori, S. *J. Biomol. NMR* **1998**, *11*, 221. (b) Melacini, G.; Boelens, R.; Kaptein, R. *J. Biomol. NMR* **1999**, *15*, 189.
- (12) Huang, L. J. S.; Taylor, S. S. *J. Biol. Chem.* **1998**, *273*, 26739.
- (13) Berman, H. M.; Ten Eyck, L. F.; Goodsell, D. S.; Haste, N. M.; Kornev, A.; Taylor, S. S. *Proc. Natl. Acad. Sci. U.S.A.* **2005**, *102*, 45.
- (14) Gibson, R. M.; Buechler, Y.; Taylor, S. S. *J. Biol. Chem.* **1997**, *272*, 16343.

JA060046D